



# Injectable Hydrogel for NIR-II Photo-Thermal Tumor Therapy and Dihydroartemisinin-Mediated Chemodynamic Therapy

Danyang Chen<sup>1†</sup>, Chuang Chen<sup>2†</sup>, Chunyu Huang<sup>1</sup>, Tongkai Chen<sup>3\*</sup> and Zeming Liu<sup>1\*</sup>

<sup>1</sup> Department of Plastic Surgery, Zhongnan Hospital of Wuhan University, Wuhan, China, <sup>2</sup> Department of Breast and Thyroid Surgery, Renmin Hospital of Wuhan University, Wuhan, China, <sup>3</sup> Science and Technology Innovation Center, Guangzhou University of Chinese Medicine, Guangzhou, China

## OPEN ACCESS

### Edited by:

Wei Cao,  
Northwestern University, United States

### Reviewed by:

Yang Mai,  
Sun Yat-sen University, China  
Junzhe Lou,  
Harvard University, United States

### \*Correspondence:

Tongkai Chen  
chentongkai@gzucm.edu.cn  
Zeming Liu  
6myt@163.com

<sup>†</sup>These authors have contributed  
equally to this work

### Specialty section:

This article was submitted to  
Nanoscience,  
a section of the journal  
Frontiers in Chemistry

Received: 12 February 2020

Accepted: 17 March 2020

Published: 07 April 2020

### Citation:

Chen D, Chen C, Huang C, Chen T  
and Liu Z (2020) Injectable Hydrogel  
for NIR-II Photo-Thermal Tumor  
Therapy and  
Dihydroartemisinin-Mediated  
Chemodynamic Therapy.  
Front. Chem. 8:251.  
doi: 10.3389/fchem.2020.00251

In traditional Chinese medicine, dihydroartemisinin (DHA) is the focus of extensive attention because of its unique activity with  $\text{Fe}^{2+}$  to produce reactive oxygen species (ROS) and promote apoptosis. In this work, we designed a newfangled ink@hydrogel containing  $\text{FeCl}_3$ , traditional Chinese ink (Hu Kaiwen ink), and agarose hydrogel to create a synergistic activity with DHA in the treatment of cancer. When the system is irradiated under 1,064 nm for a few minutes, the ink in the ink@hydrogel converts the light to heat and hyperthermia causes the reversible hydrolysis of hydrogel. Then,  $\text{Fe}^{3+}$  quickly diffuses from the hydrogel to the tumor microenvironment and is reduced to  $\text{Fe}^{2+}$  to break the endoperoxide bridge in pre-injected DHA, which results in the release of free radicals for a potent anticancer action. To our knowledge, this is the first report of a hydrogel tumor therapy system that induces a photo-thermal response in the second near infrared window (NIR-II). *in vivo* experiments also showed a significant effect of DHA- $\text{Fe}^{2+}$  in chemodynamic therapy (CDT) and in photo-thermal therapy. This hydrogel platform provided an encouraging idea for synergistic tumor therapy.

**Keywords:** injectable hydrogel, NIR-II photothermal therapy, dihydroartemisinin, Hu Kaiwen ink, chemodynamic therapy

## INTRODUCTION

Cancer is the leading cause of death worldwide and poses a huge threat to human health, even after the recent significant research advances (Li et al., 2017; Wu et al., 2018; Zhang et al., 2019). Recently, new tumor treatments, such as photothermal therapy (PTT) (Chu and Dupuy, 2014; Song et al., 2015; Sun et al., 2017; Yang et al., 2017; Jiang et al., 2018; Zhou et al., 2018; Liu et al., 2019) and chemodynamic therapy (CDT) (Jia et al., 2016), have attracted much attention due to the limited side effects and drug resistance compared with traditional strategies like chemotherapy, surgery, and radiotherapy.

The emerging PTT treatment uses nanoparticles as photo-thermal agents (PTAs) (Sun et al., 2017; Jiang et al., 2018; Cao et al., 2019; Yang et al., 2019) since they have a high absorbance in the near-infrared (NIR) to convert light to thermal energy and induce tumor ablation. PTT causes little damage to the patient and has minimal side effects. It can be used by itself or combined with other therapies like photodynamic therapy (PDT) (Hu et al., 2019; Liang et al., 2019). However, most PTAs have a limited penetration depth since they are only active in the NIR-I window (750–1,000 nm), which reduces their efficiency and clinical performance. Although NIR-II radiation (1,000–1,350 nm) (Lin et al., 2017; Yu et al., 2017; Cao et al., 2019)

has a better maximum permissible exposure (MPE) and a larger penetration depth, there is a lack of PTAs with a strong enough absorption and a high enough photo-thermal conversion efficiency. Therefore, it is necessary to explore PTAs that are active in the NIR-II window for tumor therapy. Traditional Chinese ink like the Hu Kaiwen ink has a good photo-thermal conversion efficiency, a high stability in liquid, and an excellent biocompatibility. It is therefore expected to have a great potential as an NIR-II photo-thermal material (Wang et al., 2017; Ouyang et al., 2019). Recently, light-responsive hydrogel (Xing et al., 2016; Niu et al., 2017; Hou et al., 2018; Qiu et al., 2018; Wu et al., 2019) was introduced as creative and novel drug release vessel for tumor treatment. It has attracted much attention and has a great potential for the controlled release of active agents. Furthermore, the drug release rate can be controlled by changing the power density of the incident light and the exposure time to modify the dissolution of the hydrogel. However, the photo-thermal response of hydrogels in the NIR-II spectrum has not yet been studied.

In traditional Chinese medicine, dihydroartemisinin (DHA) and its derivatives have been extensively used as an effective anti-malaria drug since the 1970s (Wang et al., 2016). Recently, they have been studied as alternative tumor therapeutic agents to kill various tumor cells *in vitro* and *in vivo* through the generation of active oxygen radicals via the homolytic cleavage of the weak endoperoxide bridge accelerated by high concentrations of ferrous ions (Wang et al., 2016). However, the insufficient availability of  $\text{Fe}^{2+}$  in the tumor tissues severely limits the clinical performance and an urgent solution is needed to increase the  $\text{Fe}^{2+}$  content in the tumor tissues and create a synergetic therapy with DHA.

Herein, we designed a newfangled ink@hydrogel containing  $\text{FeCl}_3$ , traditional Chinese ink (Hu Kaiwen ink), and agarose hydrogel to act synergistically with DHA in the treatment of cancer. When the system is irradiated at 1,064 nm for a few minutes, the ink in the ink@hydrogel converts light to heat and hyperthermia causes the reversible hydrolysis of hydrogel. Then,  $\text{Fe}^{3+}$  ions diffuse from the hydrogel to the tumor microenvironment and are reduced to  $\text{Fe}^{2+}$  to promote the breakage of the endoperoxide bridge in the pre-injected DHA. This results in the release of free radicals for a potent anticancer effect. To our best knowledge, this is the first report of a hydrogel system for tumor therapy that creates a photo-thermal response in the NIR-II biological window. *In vivo* experiments are carried out to determine the efficiency of DHA- $\text{Fe}^{2+}$  in chemodynamic therapy (CDT) and in photo-thermal therapy. This special hydrogel treatment way provided a great idea for synergistic tumor therapy.

## RESULTS AND DISCUSSION

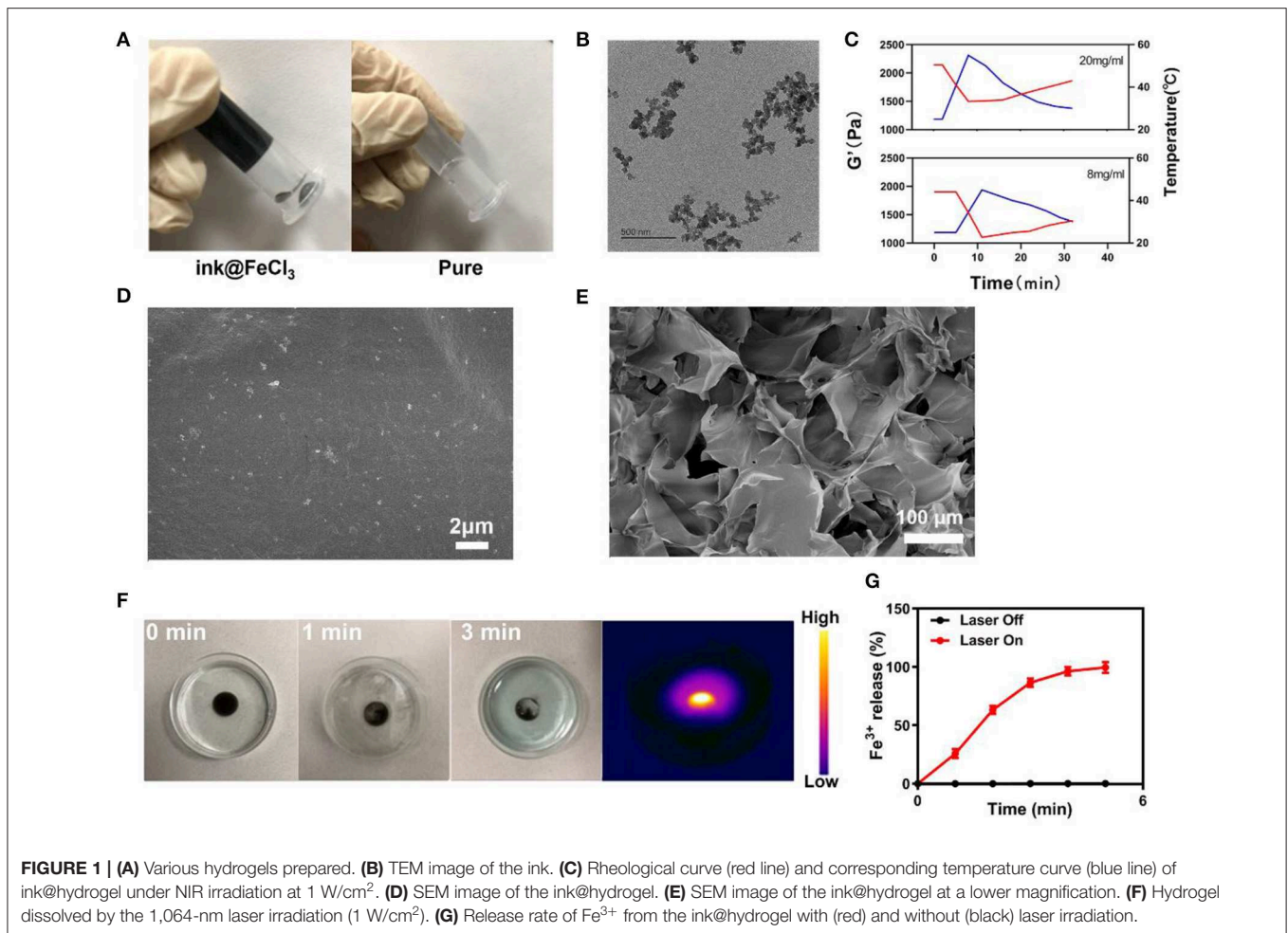
### Synthesis and Characterization of the Hydrogel

First, the ink was diluted to a light concentration to produce a usable sample. **Figure 1A** show the various hydrogels prepared. Each hydrogel was prepared in a centrifuge tube and did not flow downwards once gelation was complete. The nanoscale

morphology of the ink was determined by transmission electron microscopy (TEM) (**Figure 1B**). The ink mostly presented small aggregates. Rheology measurements on the ink@hydrogel (a mixture of agarose hydrogel and ink) with different ink concentrations showed a decrease in the storage modulus for increasing ink concentrations, as shown in **Figure 1C**. When the temperature increases, the storage modulus of the hydrogel decreases, which confirms the successful formation of the hydrogel. Representative SEM (scanning electron microscope) images of the ink@hydrogel (**Figures 1D,E**) indicated a complex pore size distribution where different concentrations and temperatures produced different pore sizes. A power density of  $1 \text{ W/cm}^2$  at 1,064 nm irradiation was used to evaluate the temperature control ability of ink@hydrogel (**Figure 1F**). Initially, the dark colors of conglomerated ink@hydrogel were observed, but persistent laser irradiation faded the colors, indicating the degradation of the ink@hydrogel. Infrared thermal imaging (**Figure 1F**) also confirmed the increase of the temperature in the ink@hydrogel upon laser irradiation. We measured the release rate of  $\text{Fe}^{3+}$  in the hydrogel with or without laser irradiation (**Figure 1G**). The ink@hydrogel gradually dissolved and released  $\text{Fe}^{3+}$  under laser irradiation at 1,064 nm ( $1 \text{ W/cm}^2$ ), whereas there was no significant change in the group without laser irradiation, which showed that the hydrogel was irradiated by laser irradiation to dissolve and release iron ions.

### Photo-Thermal of the ink@hydrogel for PTT

The photo-thermal performance of the ink was estimated by irradiating a centrifuge tube containing an aqueous ink dispersion at various concentrations (0, 10, 25, 50, and  $100 \mu\text{g/mL}$ ) with an NIR laser (1,064 nm,  $1 \text{ W/cm}^2$ ) in parallel, while capturing the infrared thermal images of the ink solutions to confirm the temperature response during irradiation (**Figures 2A,B**). The photo-thermal heating effect of the ink was concentration-dependent for a fixed irradiation power. Higher ink concentrations resulted in a greater heating effect, which indicated that the ink efficiently converted light to thermal energy. Furthermore, the temperature of the ink solution at  $100 \mu\text{g/mL}$  increased from the initial  $35^\circ\text{C}$  to nearly  $60^\circ\text{C}$  in 5 min. This suggests that the laser irradiation triggers a forceful hyperthermia and the elevated temperature is sufficient to damage tumor cells through the destruction of the intracellular protein and genetic materials. The ink solution was irradiated at 1,064 nm with  $1 \text{ W/cm}^2$  for 5 min. Then, the laser was turned off to allow the initial temperature to recover. This cycle was repeated four times (**Figure 2C**) to demonstrate that the variation of the peak temperature in every cycle was negligible and that the photo-thermal performance of the ink was stable and reproducible during cycling. The photo-thermal conversion efficiency ( $\eta$ ) of the ink was calculated from the data of **Figures 2D,F** and was as high as 35.0%, which is higher than Au nanorods (21%), graphene quantum dots (28.58%), and  $\text{Ti}_3\text{C}_2$  nanosheets (30.6%) (Liu et al., 2015; Rasool et al., 2016; Shao et al., 2016; Deng et al., 2019). **Figure 2E** shows the UV-visible-NIR absorbance spectrum of the ink solution, revealing a broad and strong absorbance between 800 and 1,100 nm, without any



obvious peak. This indicates that the hydrogel is a very suitable photo-thermal material.

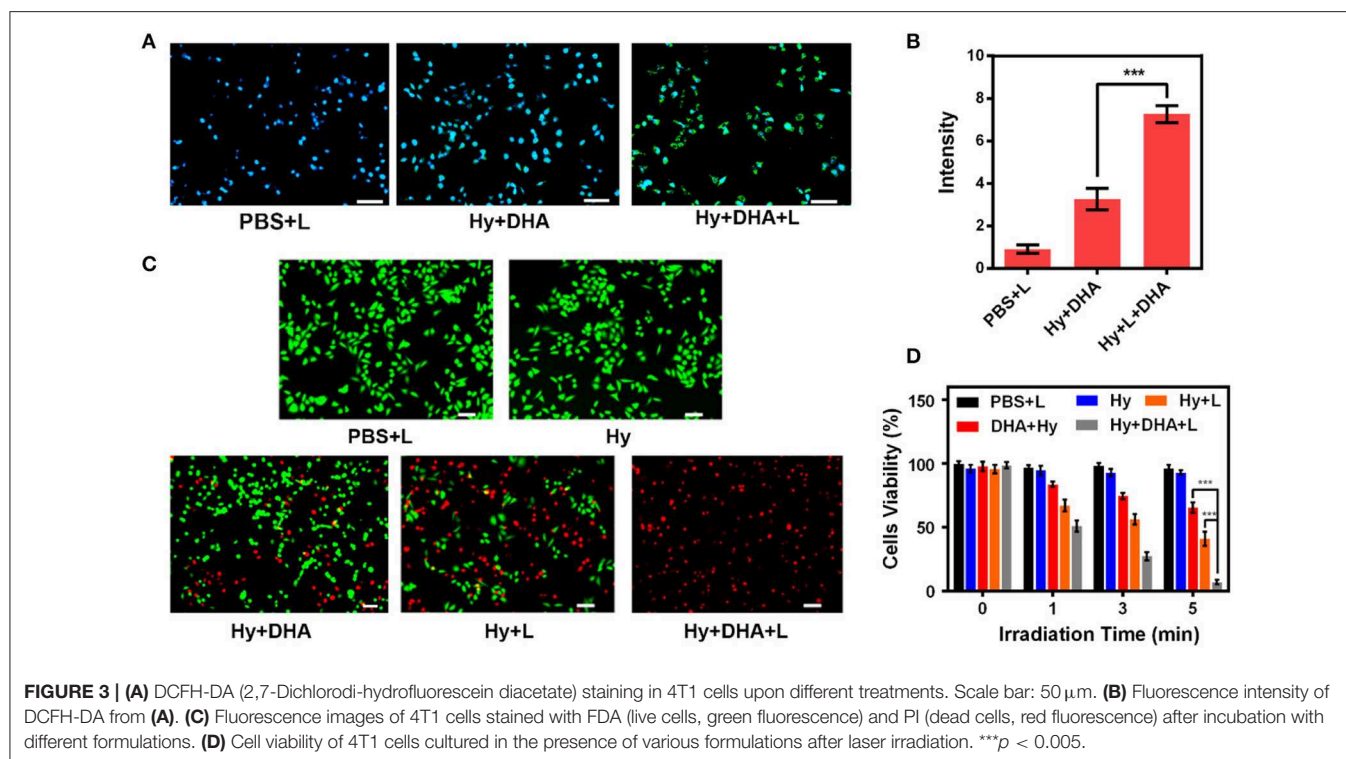
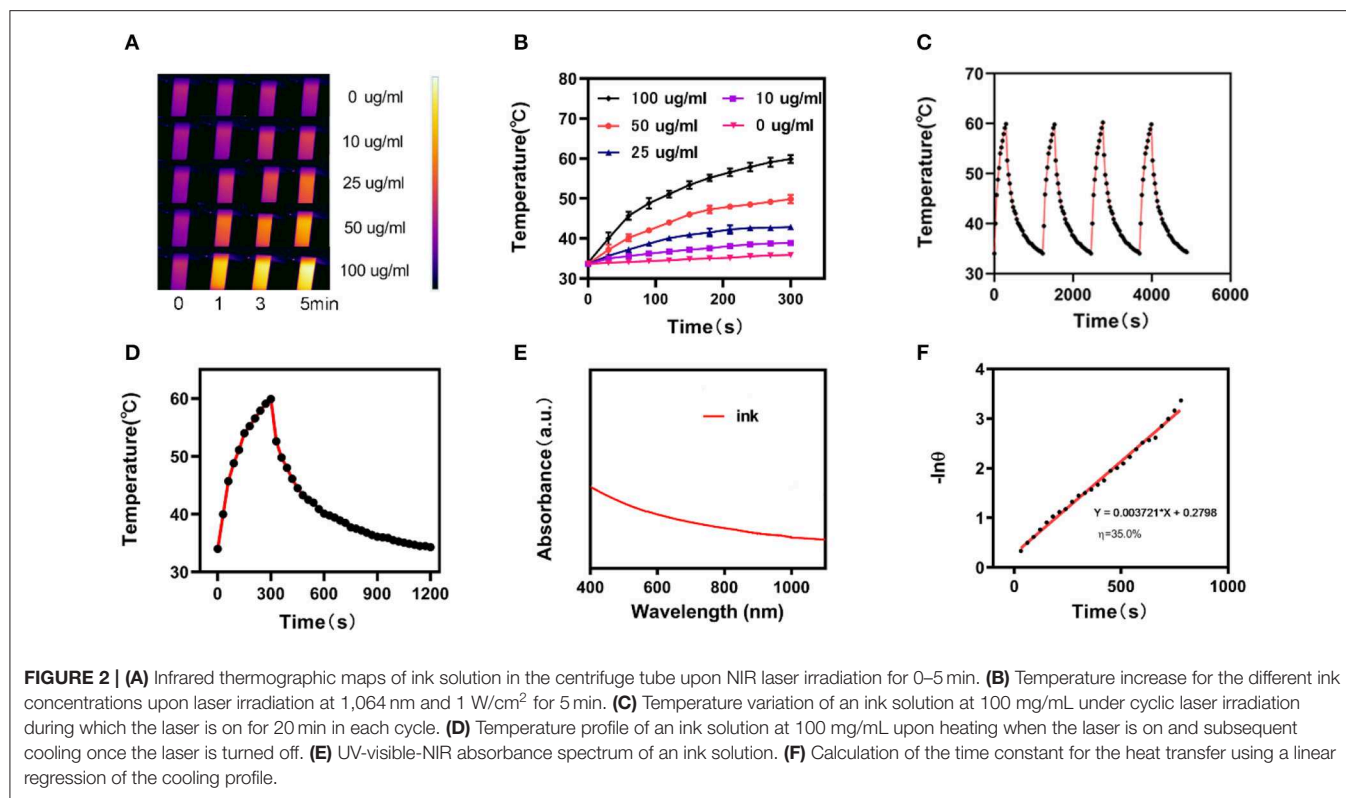
### In vitro Combination Therapy

We prepared appropriate amounts of ink@hydrogel to generate ROS *in vitro*. After the 4T1 cells were treated with different hydrogels for 2 h, the ROS stress level in the cells was measured by fluorescence microscope (Figures 3A,B). Upon laser irradiation, the ink@hydrogel samples had a high ROS level, whereas the un-irradiated hydrogel samples and irradiated PBS control had lower ROS levels. This might be attributed to the dissolution of the ink@hydrogel released Fe<sup>3+</sup> ions that were then locally reduced to Fe<sup>2+</sup>, which can be coupled with DHA. Next, we examined the fluorescence images of the 4T1 cells stained with FDA (Fluorescein diacetate) (live cells, green fluorescence) and PI (propidium iodide) (dead cells, red fluorescence) under different conditions (Figure 3C). By comparing the images of the ink@hydrogel group with or without laser irradiation, the viability of the 4T1 cells significantly decreased upon laser irradiation most likely due to the temperature increase that triggers the dissolution of the hydrogel and releases Fe<sup>3+</sup> ions. The group with ink@hydrogel and DHA subjected to the laser

irradiation showed a high level of apoptosis due to the generation of hydroxyl radicals from the breakage of endoperoxide bridges during the action of DHA and Fe<sup>2+</sup>. Figure 3D later confirmed the cell toxicity of the hydrogel with DHA upon laser irradiation. The cells incubated with hydrogel were damaged and died after 5 min of laser irradiation.

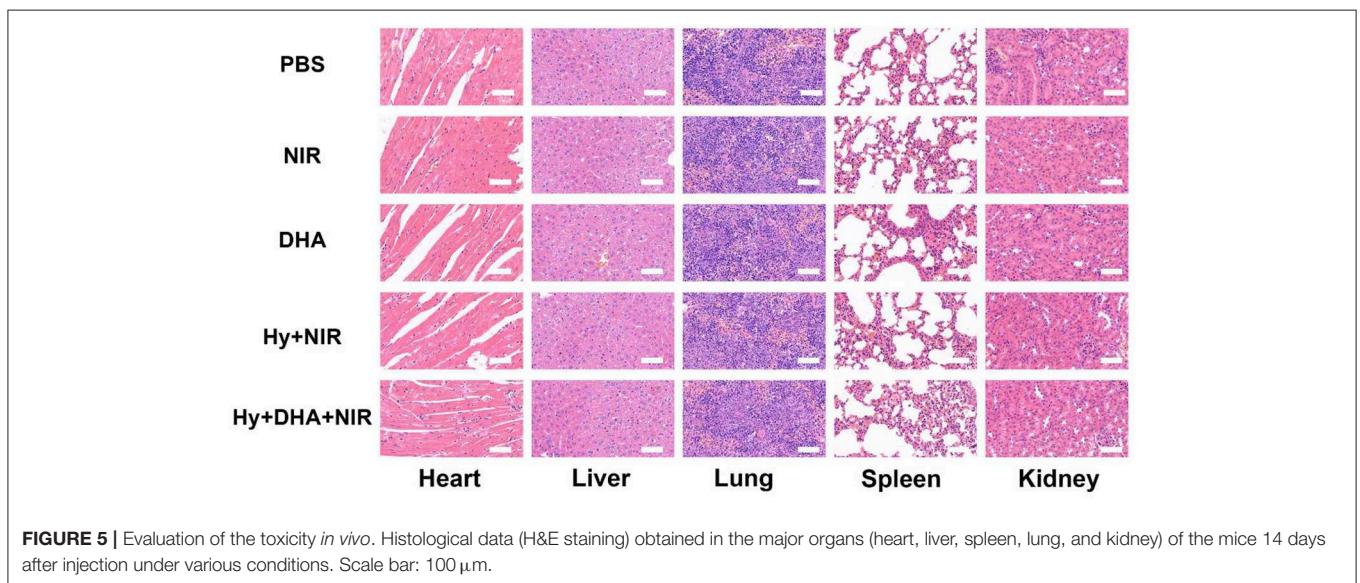
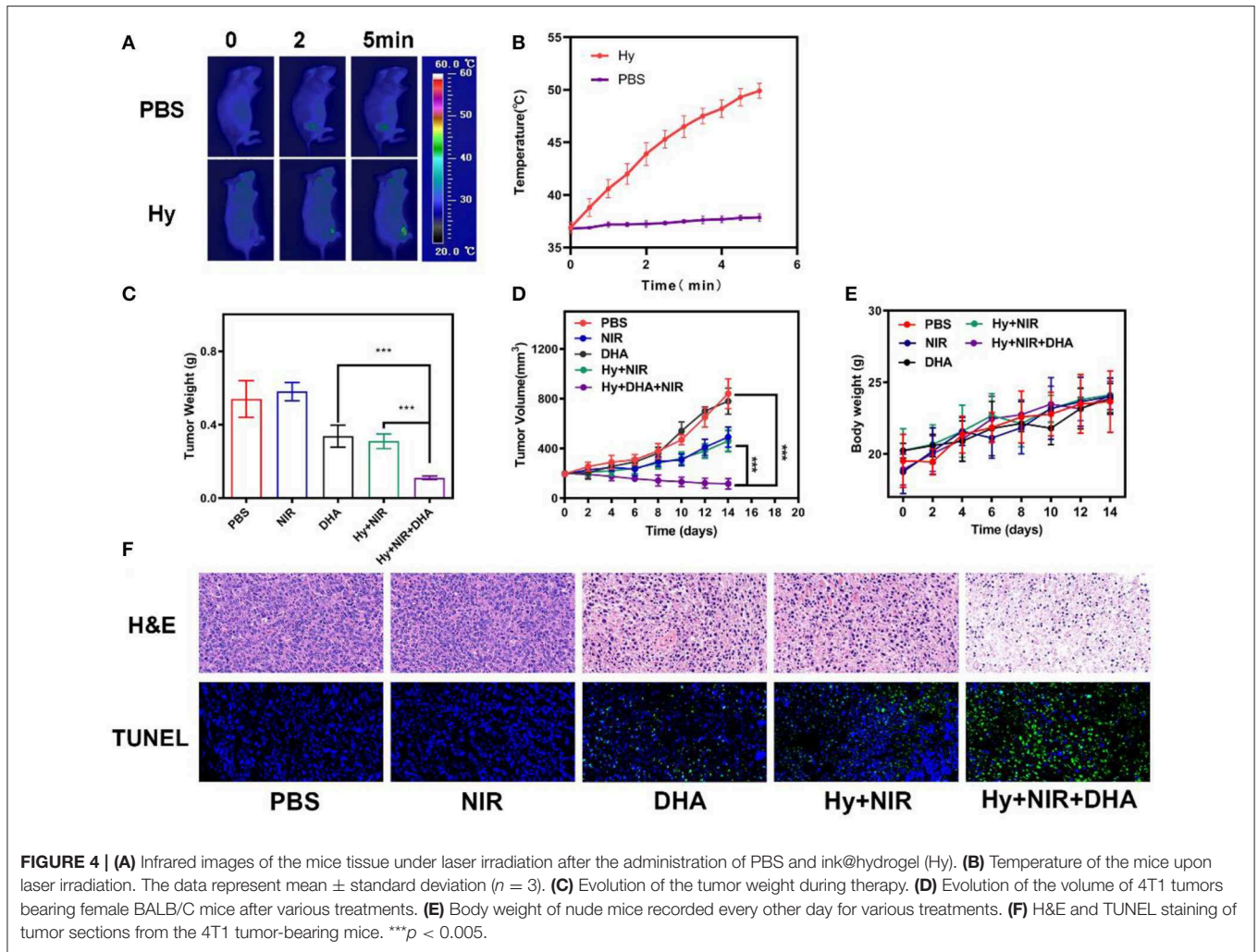
### In vivo Anti-tumor Study

Since the *in vitro* results were very encouraging for the ink@hydrogel combined with DHA, we studied the *in vivo* potential. Mice bearing 4T1 tumors were split into five groups when the tumor volume reached ≈200 mm<sup>3</sup> ( $n = 5$ ): (1) PBS solution group, (2) laser irradiation group, (3) 5 mg/kg DHA solution group, (4) ink@hydrogel with laser irradiation, (5) ink@hydrogel and DHA with laser irradiation. The five groups significantly demonstrated the efficiency of a therapy using hydrogel combined with DHA and laser irradiation. DHA was administered by intra-peritoneal injection whereas the other solutions were administered by orthotopic injection. DHA was injected 12 h before the ink@hydrogel. Figure 4A shows an infrared image of the PBS group and the hydrogel with DHA group under laser irradiation. The temperature in the



control group barely increased, whereas the *in vivo* temperature distribution in the ink@hydrogel with DHA group was raised by about 15°C in 5 min (Figure 4B). The reduced heat tolerance

of the tumor tissue compared to normal cells results in the selective destruction of the tumor cells at temperatures above hyperthermia (42–47°C) (Yang et al., 2017). The volume of the



tumors in each of the five groups was measured every other day using a digital caliper and the tumor weight was calculated, as shown in **Figures 4C,D**. Compared with the PBS and NIR irradiation group, the tumor grew slowly in the DHA group and the ink@hydrogel without DHA group under laser irradiation. The volume and the weight of the tumor in the hydrogel with DHA group were significantly lowered as the average mice weight in hydrogel with DHA group were only 0.11 g. The body-weight regularly increased in all groups during the whole therapy (**Figure 4E**), which confirmed that these treatments produced negligible adverse effects on the mice. We also examined the micrographs of tumor tissues stained with H&E and TUNEL (**Figure 4F**). The combination of the photo-thermal therapy with DHA yielded the highest apoptosis rate for the tumor cells.

## Histological Analysis

We performed a histological analysis of the major organs (heart, liver, spleen, lung, and kidney) for the ink@hydrogel combined with DHA group (**Figure 5**). The results indicated that the synergistic ink@hydrogel and DHA therapy did not cause deep pathological changes in the organs, suggesting that there was no significant histological abnormality in the treatment groups.

## CONCLUSION

In summary, we designed a newfangled ink@hydrogel system, which can produce a synergistic activity with DHA for the treatment of cancer. The ink in the ink@hydrogel could generate huge heat energy and hyperthermia when under 1064 nm laser irradiation as it possessed good photothermal performance and stability. Furthermore, Hu Kaiwen ink as an NIR-II photothermal material has great maximum permissible exposure (MPE) and a larger penetration depth. Then,  $\text{Fe}^{3+}$  ions rapidly diffused from the hydrogel to the tumor microenvironment

## REFERENCES

- Cao, Y., Wu, T., Zhang, K., Meng, X., Dai, W., Wang, D., et al. (2019). Engineered exosome-mediated near-infrared-II region V2C quantum dot delivery for nucleus-target low-temperature photothermal therapy. *ACS Nano* 13, 1499–1510. doi: 10.1021/acsnano.8b07224
- Chu, K. F., and Dupuy, D. E. (2014). Thermal ablation of tumours: biological mechanisms and advances in therapy. *Nat. Rev. Cancer* 14, 199–208. doi: 10.1038/nrc3672
- Deng, X., Liang, S., Cai, X., Huang, S., Cheng, Z., Shi, Y., et al. (2019). Yolk-shell structured au nanostar@metal-organic framework for synergistic chemophotothermal therapy in the second near-infrared window. *Nano Lett.* 19, 6772–6780. doi: 10.1021/acs.nanolett.9b01716
- Hou, M., Yang, R., Zhang, L., Zhang, L., Liu, G., Xu, Z., et al. (2018). Injectable and natural humic acid/agarose hybrid hydrogel for localized light-driven photothermal ablation and chemotherapy of cancer. *ACS Biomater. Sci. Eng.* 4, 4266–4277. doi: 10.1021/acsbomaterials.8b01147
- Hu, J. J., Chen, Y., Li, Z. H., Peng, S. Y., Sun, Y., and Zhang, X. Z. (2019). Augment of oxidative damage with enhanced photodynamic process and MTH1 inhibition for tumor therapy. *Nano Lett.* 19, 5568–5576. doi: 10.1021/acs.nanolett.9b02112
- Jia, H. R., Wang, H. Y., Yu, Z. W., Chen, Z., and Wu, F. G. (2016). Long-time plasma membrane imaging based on a two-step synergistic cell surface modification strategy. *Bioconjug. Chem.* 27, 782–789. doi: 10.1021/acs.bioconjugchem.6b00003
- Jiang, W., Zhang, H., Wu, J., Zhai, G., Li, Z., Luan, Y., et al. (2018). CuS@MOF-based designed well-designed quercetin delivery system for chemophotothermal therapy. *ACS Appl. Mater. Interfaces* 10, 34513–34523. doi: 10.1021/acsami.8b13487
- Li, S. Y., Cheng, H., Xie, B. R., Qiu, W. X., Zeng, J. Y., Li, C. X., et al. (2017). Cancer cell membrane camouflaged cascade bioreactor for cancer targeted starvation and photodynamic therapy. *ACS Nano* 11, 7006–7018. doi: 10.1021/acsnano.7b02533
- Liang, S., Deng, X., Chang, Y., Sun, C., Shao, S., Xie, Z., et al. (2019). Intelligent hollow Pt-CuS janus architecture for synergistic catalysis-enhanced sonodynamic and photothermal cancer therapy. *Nano Lett.* 19, 4134–4145. doi: 10.1021/acs.nanolett.9b01595
- Lin, H., Gao, S., Dai, C., Chen, Y., and Shi, J. (2017). A two-dimensional biodegradable niobium carbide (MXene) for photothermal tumor eradication in NIR-I and NIR-II biowindows. *J. Am. Chem. Soc.* 139, 16235–16247. doi: 10.1021/jacs.7b07818
- Liu, C., Xing, J., Akakuru, O. U., Luo, L., Sun, S., Zou, R., et al. (2019). Nanozymes-engineered metal-organic frameworks for catalytic cascades-enhanced synergistic cancer therapy. *Nano Lett.* 19, 5674–5682. doi: 10.1021/acs.nanolett.9b02253
- Liu, Y., Ashton, J. R., Moding, E. J., Yuan, H., Register, J. K., Fales, A. M., et al. (2015). A plasmonic gold nanostar theranostic probe for *in vivo* tumor imaging and photothermal therapy. *Theranostics* 5, 946–960. doi: 10.7150/thno.11974
- Niu, X., Zhang, Z., and Zhong, Y. (2017). Hydrogel loaded with self-assembled dextran sulfate-doxorubicin complexes as a delivery system with dissolution of ink@hydrogel and were reduced to  $\text{Fe}^{2+}$  to promote the breakage of the endoperoxide bridges in the previously-injected DHA. This resulted in the release of free radicals for a potent anti-cancer effect. And the drug release rate can be controlled by changing different condition. *In vitro* and *in vivo* experiments illustrated the great therapeutic effect of DHA- $\text{Fe}^{2+}$ . To our best knowledge, this is the first report of a hydrogel tumor therapy system that generates a photo-thermal response in the NIR-II window. We envisioned that this special hydrogel treatment way holds great potential in synergistic tumor therapy.

## DATA AVAILABILITY STATEMENT

All datasets generated for this study are included in the article/supplementary material.

## ETHICS STATEMENT

The animal study was reviewed and approved by Wuhan University Animal Care Facility.

## AUTHOR CONTRIBUTIONS

DC and CC performed the experiments, analyzed all the data, drafted all the figures, and prepared the manuscript. CH performed the experiments. TC and ZL conceived, designed the experiments, and revised the manuscript.

## FUNDING

This work was supported by the Independent Research Project of Wuhan University (znpzy2018094) and the Fundamental Research Funds for the Central Universities (2042019kf0229).

- for chemotherapy. *Mater. Sci. Eng. C Mater. Biol. Appl.* 77, 888–894. doi: 10.1016/j.msec.2017.04.013
- Ouyang, B., Liu, F., Ruan, S., Liu, Y., Guo, H., Cai, Z., et al. (2019). Localized free radicals burst triggered by NIR-II light for augmented low-temperature photothermal therapy. *ACS Appl. Mater. Interfaces* 11, 38555–38567. doi: 10.1021/acsami.9b15009
- Qiu, M., Wang, D., Liang, W., Liu, L., Zhang, Y., Chen, X., et al. (2018). Novel concept of the smart NIR-light-controlled drug release of black phosphorus nanostructure for cancer therapy. *Proc. Natl. Acad. Sci. U.S.A.* 115, 501–506. doi: 10.1073/pnas.1714421115
- Rasool, K., Helal, M., Ali, A., Ren, C. E., Gogotsi, Y., and Mahmoud, K. A. (2016). Antibacterial activity of Ti(3)C(2)Tx MXene. *ACS Nano* 10, 3674–3684. doi: 10.1021/acsnano.6b00181
- Shao, J., Xie, H., Huang, H., Li, Z., Sun, Z., Xu, Y., et al. (2016). Biodegradable black phosphorus-based nanospheres for *in vivo* photothermal cancer therapy. *Nat. Commun.* 7:12967. doi: 10.1038/ncomms12967
- Song, G., Liang, C., Gong, H., Li, M., Zheng, X., Cheng, L., et al. (2015). Core-shell MnSe@Bi<sub>2</sub>Se<sub>3</sub> fabricated via a cation exchange method as novel nanotheranostics for multimodal imaging and synergistic thermoradiotherapy. *Adv. Mater.* 27, 6110–6117. doi: 10.1002/adma.201503006
- Sun, H., Su, J., Meng, Q., Yin, Q., Chen, L., Gu, W., et al. (2017). Cancer cell membrane-coated gold nanocages with hyperthermia-triggered drug release and homotypic target inhibit growth and metastasis of breast cancer. *Adv. Funct. Mater.* 27:1604300. doi: 10.1002/adfm.201604300
- Wang, D., Zhou, J., Chen, R., Shi, R., Xia, G., Zhou, S., et al. (2016). Magnetically guided delivery of DHA and Fe ions for enhanced cancer therapy based on pH-responsive degradation of DHA-loaded Fe<sub>3</sub>O<sub>4</sub>@C@MIL-100(Fe) nanoparticles. *Biomaterials* 107, 88–101. doi: 10.1016/j.biomaterials.2016.08.039
- Wang, S., Cao, Y., Zhang, Q., Peng, H., Liang, L., Li, Q., et al. (2017). New application of old material: chinese traditional ink for photothermal therapy of metastatic lymph nodes. *ACS Omega* 2, 5170–5178. doi: 10.1021/acsomega.7b00993
- Wu, H., Liu, L., Song, L., Ma, M., Gu, N., and Zhang, Y. (2019). Enhanced tumor synergistic therapy by injectable magnetic hydrogel mediated generation of hyperthermia and highly toxic reactive oxygen species. *ACS Nano* 13, 14013–14023. doi: 10.1021/acsnano.9b06134
- Wu, M. X., Yan, H. J., Gao, J., Cheng, Y., Yang, J., Wu, J. R., et al. (2018). Multifunctional supramolecular materials constructed from polypyrrole@UiO-66 nanohybrids and pillararene nanovalves for targeted chemophotothermal therapy. *ACS Appl. Mater. Interfaces* 10, 34655–34663. doi: 10.1021/acsami.8b13758
- Xing, R., Liu, K., Jiao, T., Zhang, N., Ma, K., Zhang, R., et al. (2016). An injectable self-assembling collagen-gold hybrid hydrogel for combinatorial antitumor photothermal/photodynamic therapy. *Adv. Mater.* 28, 3669–3676. doi: 10.1002/adma.201600284
- Yang, J., Xie, R., Feng, L., Liu, B., Lv, R., Li, C., et al. (2019). Hyperthermia and controllable free radical coenhanced synergistic therapy in hypoxia enabled by near-infrared-II light irradiation. *ACS Nano* 13, 13144–13160. doi: 10.1021/acsnano.9b05985
- Yang, Y., Zhu, W., Dong, Z., Chao, Y., Xu, L., Chen, M., et al. (2017). 1D coordination polymer nanofibers for low-temperature photothermal therapy. *Adv. Mater.* 29:1703588. doi: 10.1002/adma.201703588
- Yu, X., Li, A., Zhao, C., Yang, K., Chen, X., and Li, W. (2017). Ultrasmall semimetal nanoparticles of bismuth for dual-modal computed tomography/photoacoustic imaging and synergistic thermoradiotherapy. *ACS Nano* 11, 3990–4001. doi: 10.1021/acsnano.7b00476
- Zhang, F., Liu, Y., Lei, J., Wang, S., Ji, X., Liu, H., et al. (2019). Metal-organic-framework-derived carbon nanostructures for site-specific dual-modality photothermal/photodynamic thrombus therapy. *Adv. Sci.* 6:1901378. doi: 10.1002/advs.201901378
- Zhou, J., Jiang, Y., Hou, S., Upputuri, P. K., Wu, D., Li, J., et al. (2018). Compact plasmonic blackbody for cancer theranosis in the near-infrared II window. *ACS Nano* 12, 2643–2651. doi: 10.1021/acsnano.7b08725

**Conflict of Interest:** The authors declare that the research was conducted in the absence of any commercial or financial relationships that could be construed as a potential conflict of interest.

Copyright © 2020 Chen, Chen, Huang, Chen and Liu. This is an open-access article distributed under the terms of the Creative Commons Attribution License (CC BY). The use, distribution or reproduction in other forums is permitted, provided the original author(s) and the copyright owner(s) are credited and that the original publication in this journal is cited, in accordance with accepted academic practice. No use, distribution or reproduction is permitted which does not comply with these terms.